TD-03-008
03/03

ANALYSIS OF THE B2 CORRECTION IN THE TEVATRON

G. Annala*, P. Bauer[1], J. DiMarco, R. Hanft, M. Lamm,
M. Martens*, P. Schlabach, J. Tompkins, G. Velev
Fermilab, Technical Division
* Fermilab, Beams Division

Beam loss and emittance dilution during ramping from injection to collision energy is observed in the Tevatron, now in its collider run-II stage. This phenomenon is believed to be related mostly to beam instabilities. There has been, however, repeated expression of concern that imperfect control of the machine chromaticity during the injection porch and the ensuing ramp to collision could also contribute to the beam loss. It is well known that the magnetic multipoles and most importantly the sextupole component in the superconducting dipole magnets in the Tevatron decay during the injection plateau and snap back to the value before the start of the decay at the start of the ramp. Sextupole correctors distributed around the ring are used to counteract the sextupole decay in the main magnets. To determine if the sextupole compensation is working successfully in the Tevatron a thorough investigation of the Tevatron chromaticity settings and corrections was conducted and compared to the results of magnetic measurements performed on magnets. The following reports on the results of this investigation, showing that the sextupole decay and snapback are compensated to within a fraction of a unit with the current Tevatron chromaticity correction scheme. Although some minor, possible improvements are discussed, this note supports the status quo as no basic inconsistency was found in the Tevatron sextupole correction scheme. These findings were also confirmed by chromaticity measurements performed on the beam, which are reported in this note.

[1] e-mail: pbauer@fnal.gov

1) Dynamic Effects in Superconducting Magnets

It is well known that the magnetic multipoles and most importantly the sextupole (b_2) component in the superconducting dipole magnets in the Tevatron decay by approximately one unit (defined as 10^{-4} of the main dipole field in the bore and measured at the reference radius of 25.4 mm) during the injection plateau, [1]. Also at the beginning of the ramp the sextupole quickly snaps back to the initial level before the decay (while at the same time evolving along the hysteretic loop). These effects were first discovered in the Tevatron. Figure 1 shows the hysteretic sextupole in a Tevatron dipole magnet (TC0504), together with the dynamic effects mentioned above. The hysteretic b_2 evolves around the so-called geometric b_2. The geometric b_2 in the example of Figure 1 is 13 units. The average geometric b_2 of all installed Tevatron dipoles is 1.47 units [2]. The geometric b_2 is more or less independent of field in the Tevatron dipoles because saturation effects are small and Lorentz-forces (which can lead to geometrical deformations at high currents) are moderate.

Qualitative models exist that help to explain the dynamic effects observed in superconducting magnets. These models assume that current imbalances between the strands in the cable of the Tevatron dipole magnet produce sinusoidal field variations along the cables with a period equal to the twist pitch of the strands in the cable. The current imbalances, caused for example by varying splice to strand resistances or spatially varying dB/dt in the magnet ends, vary only slowly with time (time constants of thousands of seconds) because of the fact that current redistribution is not favored given that the currents are running for the most part in zero resistance superconductor. The time constant depends strongly on the distribution of (cross and adjacent) contact resistances along the cable in the coils. The drift effects found in the magnetic multipoles are a direct consequence of the local field variations seen by the strands as a result of the slowly decaying current imbalances. During ramping of the magnet these field variations do not

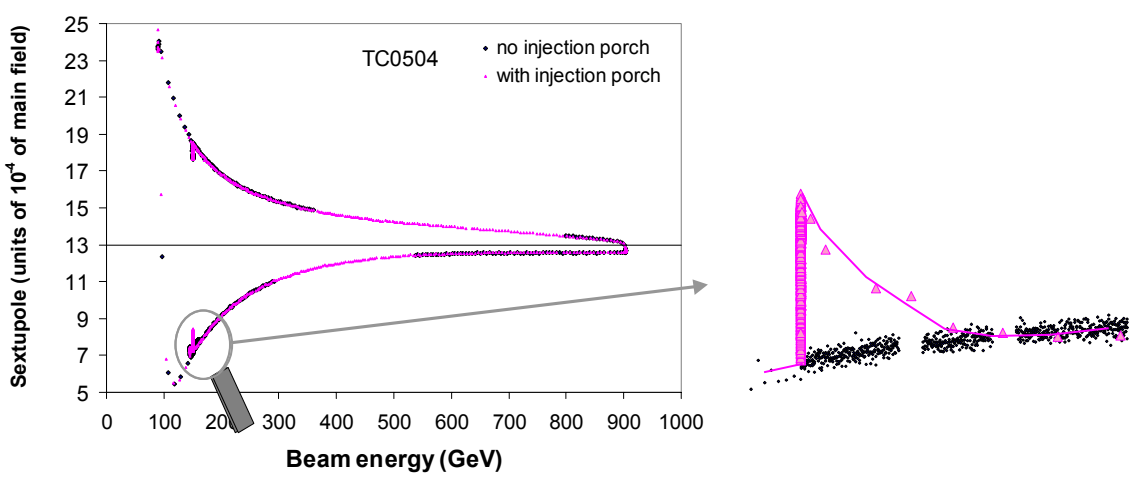

Figure 1: Example of b_2 (at 25.4 mm radius) drift and snapback in Tevatron model TC0504 ([3]). The right plot is a blow-up of the drift and snapback during and after injection. For comparative purposes measurements with and without dwell at injection are shown.

affect the cross-sectional multipole distribution. At constant excitation, however, the hysteretic nature of the magnetization of the strands together with the time varying current redistribution within the cable produce the dynamic behavior of the cross-sectional multipole pattern that can be seen in Figure 1.

2) Sextupole Decay and Snapback Compensation Algorithm

The sextupole drift and snapback in Tevatron magnets are corrected using the sextupole corrector circuits. Note that the b_2 correction scheme described here addresses only the b_2 drift and ensuing snapback, which play out on top of the more conventional b_2 characteristics in the dipole magnets (hysteretic and geometric). The currently used decay and snapback compensation currents for the chromaticity corrector circuits are calculated from fits of the sextupole decay and snapback measured on Tevatron dipoles in 1996 [3]. A thorough description of the b_2 compensation algorithm was also recently published in [4]. The fits also represent characteristics of the drift and snapback patterns in Tevatron magnets established in former measurement campaigns (see for example reference [5] for further details regarding former magnet studies). These fits as a function of different pre-cycle parameters are given in the following. Note that there is a slight disagreement between the fits presented here or in [4] and those discussed in [3]. This difference, which is a difference in the constants, not in form, reflects beam-based adjustments of the formalism. A quantitative estimate of the beam-based adjustments is given in chapter 4. Also note that the algorithms and more precisely the parameters of the algorithm depend on the particular accelerator powering waveform, which is assumed to be the current collider run-II waveform. Schematic 1 shows the basic layout of the Tevatron waveform, including the pre-cycle. The history parameters of the fit are the flat-top time and back-porch time of the pre-cycle. The injection current is 663 A (0.66 T dipole field, 150 GeV beam energy) and the flat-top current is 4333 A (4.3 T, 980 GeV). The magnetization reset is performed at 90 GeV. Given the powering history dependence of dynamic effects the pre-cycle serves to bring all magnets into a similar magnetic state.
The sextupole decay (in units of the main dipole at 25.4 mm), which is fed to the sextupole corrector circuits, as a function of plateau time at the back-porch t_{ext} and flat-top time t_{ft} for a standard Tevatron powering cycle is given as a function of the time at the injection porch (all time parameters are in seconds):

$$b_2\left(t_{ext}, t_{ft}, t\right) = b_2^{ini}\left(t_{ext}, t_{ft}\right) + m\left(t_{ext}, t_{ft}\right)\ln(t) \quad units\ at\ 25.4\ mm, \tag{1}$$

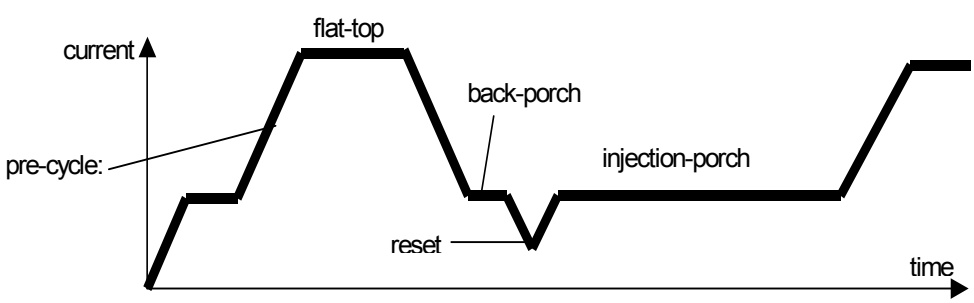

Schematic 1: Tevatron pre-cycle, injection porch and ramp to collision.

where the initial sextupole (in units at 25.4 mm) at injection (the so called intercept) before the start of the decay is given with:

$$b_2^{ini}\left(t_{ext},t_{ft}\right)=-A\ln\left(\frac{t_{ext}}{60}\right)-\left[B-C\ln\left(\frac{t_{ext}}{60}\right)\right]\ln\left(t_{ft}\right)\quad units\ at\ 25.4\ mm\ . \tag{2}$$

The scaling constant m (the slope of the decay in units/decade) as a function of extraction and flat-top time is:

$$m\left(t_{ext},t_{ft}\right)=D-E\cdot\left[2\ln\left(t_{ext}\right)-\ln\left(t_{ft}\right)\right], \tag{3}$$

The parameters of the intercept and slope fits, (2) and (3), are listed in Table 1.

Table 1: Parameters of sextupole decay algorithm presently used in the Tevatron, equ. (2) & (3).

Parameter	A	B	C	D	E
Tevatron	0.04	0.161	0.0277	0.342	0.0208

and the snapback compensation (as a function of the snapback duration t_{sb}) is:

$$b_2^{snap}\left(t_{ext},t_{ft},t_{inj},t_{sb},t\right)=b_2\left(t_{ext},t_{ft},t_{inj}\right)\left[1-\left(\frac{t}{t_{sb}}\right)^2\right]^2\quad units\ at\ 25.4\ mm, \tag{4}$$

where $b_2(t_{ext},t_{ft},t_{inj})$ is the sextupole (in units) at the end of the injection porch (at $t=t_{inj}$), as calculated from the decay fit (1) and t_{sb} is the duration of the snapback (which is 6 sec for the current Tevatron ramp).
A total of 176 sextupole correctors, in two families (SD, SF) distributed in alternating sequence around the ring are injected with a current to compensate the sextupole decay as well as the ensuing snapback (to the initial level before the decay) at the start of the ramp. The sextupole correctors are placed next to the quadrupoles at the end of each cell. The SF units are located in horizontally focusing regions (where β_x is large), therefore having a large effect on the horizontal chromaticity. The SD units are in vertically focusing regions (where β_y is large), therefore having a large effect on the vertical chromaticity. Equations (5) and (6) give the relation between sextupole corrector current and b_2 in the dipoles needed for the compensation. The coefficients were measured in the Tevatron. Appendix 1 gives a complete derivation of (5) and (6). There is a small discrepancy between the calculated coefficients in appendix 1 and the measured coefficients in (5) and (6).

$$I_{T:SFB2}(t)=-0.4964\,b_2(units)\quad (A) \tag{5}$$

$$I_{T:SDB2}(t)=-0.765\,b_2(units)\quad (A) \tag{6}$$

3) Comparison of Decay & Snapback Fit and Magnet Data – Part I

Figure 2 compares the b_2 calculated with (1)-(4) with the sextupole decay and snapback measured on magnet TC1052 in 1996 [3] for a 1 min back-porch and a 10 min flat-top pre-cycle. The fit was formulated on the basis of magnetic measurements obtained on this particular magnet. Since the Tevatron fit is based on TC1052 data, good agreement is expected between fit and magnetic measurements. Note, however, that in general the degree of agreement between the Tevatron b_2-fit and the b_2 measured on a particular magnet is not necessarily of any significance, since the Tevatron fit should represent the average of all dipole magnets installed in the ring. Given the magnet-to-magnet spread in dynamic b_2 characteristics it is unlikely that any particular magnet will exactly match the Tevatron fit. This will be discussed in further detail in chapter 6. Such a comparison, however, is an interesting exercise that should be conducted in order to give a first impression of the functional shape of the algorithm used to compensate for dynamic effects in Tevatron magnets. The measurement data in Figure 2 were offset corrected, i.e. the geometric (13 units) and the hysteretic magnetization (-4.4 units) b_2 at 150 GeV were subtracted from the data, such as to show the decay and snapback only (also the growth of hysteretic b_2 during the snapback has been corrected for). No temperature correction was applied (because it is not clear at that point how dynamic effects behave with temperature), although there is a discrepancy between the average magnet temperature in the Tevatron (currently ~4 K [8]) and the temperature at which the measurement on TC1052 was performed (~4.5 K). Furthermore, the fit uses parameters (listed in Table 1) that were derived on the basis of measurements with a 900 GeV flat-top energy in the pre-cycle, while the pre-cycle flat-top in the Tevatron today is 980 GeV. Also, in the case

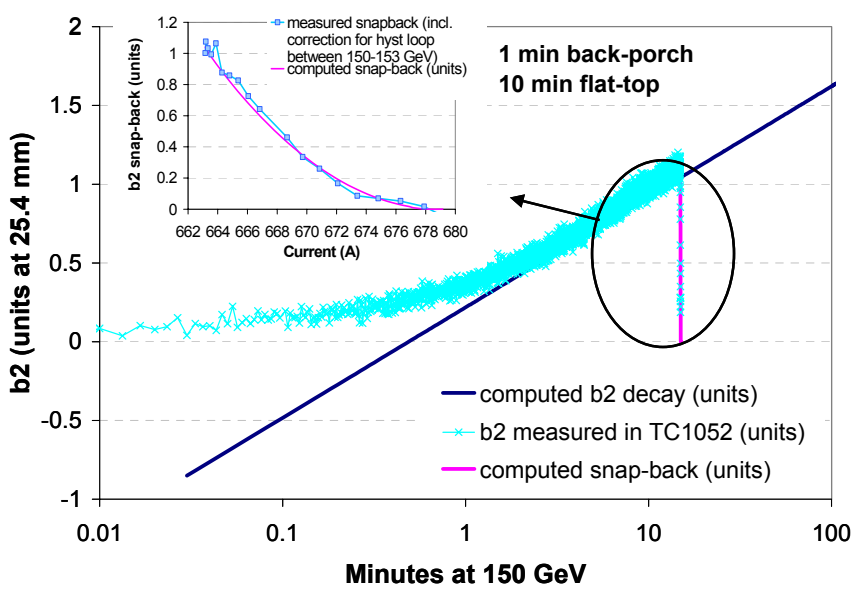

Figure 2: Comparison of decay compensation algorithm for Tevatron injection and magnetic measurements on TC1052 reported in [3]. Measurements on TC1052 were performed with 10 min at flat-top and 1 min on back-porch (2 pre-cycles). The insert shows a zoom into the snapback region. The snapback is plotted as a function of current.

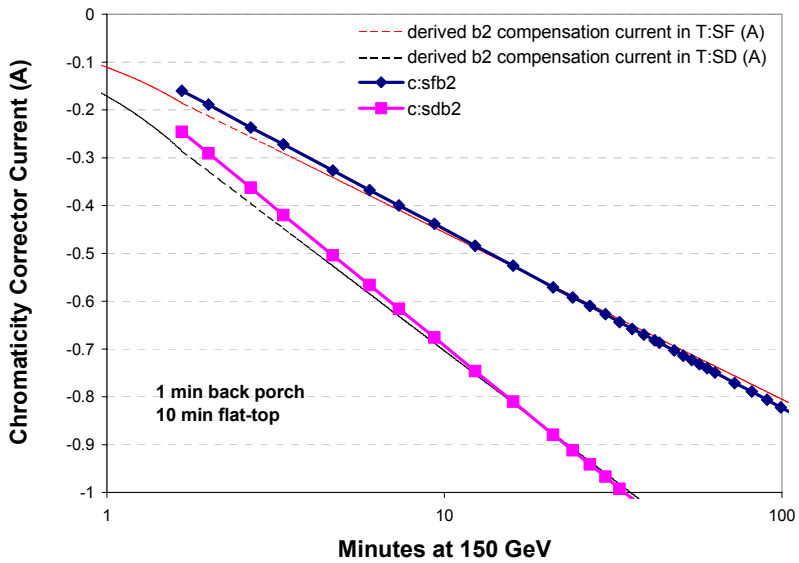

Figure 3: Sextupole currents calculated from equations (1)-(6) and as used in the Tevatron (on the basis of the same fit). T:SFB2 and T:SDB2 settings were taken for Tevatron run 1766 (Sept. 18th 2002).

of the insert showing the snapback as a function of current, the hysteretic b_2 was subtracted from the measured snapback data such as to show the pure snapback (in TC1052 the slope of the b_2-hysteresis loop is approximately linear with a slope $k_{b2}=0.00935$ *units/A*). The calculated b_2 (equ.1-4) fit the experimental data very well (at least in a relative sense). If one would include the flat-top energy corrections (see a discussion in chapter 4 and appendix 3) a larger discrepancy between the fit and the modified TC1052 data would appear in Figure 2. There is, however, a large discrepancy at times smaller than one minute. This is the result of an offset of ~-1 unit in the calculated b_2 that allows for a good fit of the data at $t>1$ *min*. This is required to allow a fit of the data with a one-time constant logarithmic function. The experimental data available (including recent data discussed in [7]) are not conclusive regarding the particular shape of the sextupole drift in the average Tevatron dipole. In magnet TC1052, however, a model with at least two time constants, one for $t<1min$ and another for $t>1min$, would be more appropriate. It is noteworthy that the discrepancy at small times does not affect the Tevatron operation because: -1- the beam is never injected before several minutes on injection porch, -2- the current table for the sextupole correction (T:SFB2 and T:SDB2) automatically sets the current to zero at $t=0$ (where the logarithmic function diverges). The current at the next time point in the current table is computed from the b_2 algorithm ((1)-(4)) and the corrector current – b_2 conversion ((5)-(6)) at 1.667 min. The correction currents fed into the SF and SD sextupole correctors (which are calculated from the b_2 fit) are shown in Figure 3 together with currents extracted from the Tevatron tables for a particular run (Tev run 1776). The calculated and measured data compare reasonably well. As indicated above the calculated currents do not follow a straight line as expected from (1)-(3) and (5)-(6). That is because they are force-fitted to reach zero at $t=0$ and interpolated linearly between zero and the current

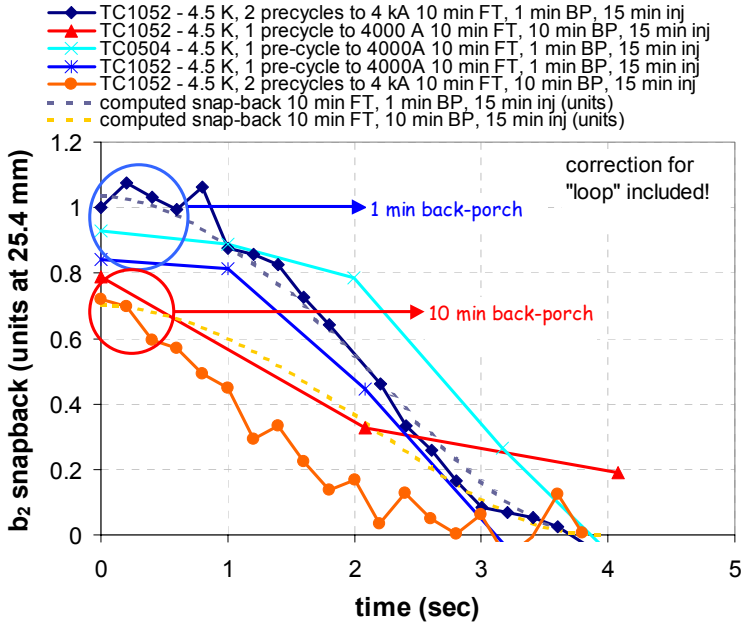

Figure 4: Comparison of snapbacks measured on TC1052 and TC0504 and the calculated snapback based on the Tevatron snapback fit (equ. 4). Note that the magnetic measurements were performed with the Tev96 ramp, such that the snapback time is 4 sec. The same snapback time was used in the fit. Also the magnet data are corrected for the increase in hysteretic b_2 during the snapback. The Tevatron 96 ramp is shown together with the current Tevatron ramp in Figure 28 in appendix 1.

computed at the first time point at $t=1.667\ min$. Figure 4 shows several different snapbacks measured in 96 in two different magnets with different pre-cycle parameters. Although there is considerable scatter in the data the duration of the snapback is almost constant at ~4 sec. Also the agreement between the magnet data and the fit is satisfactory. The effect of back-porch duration can clearly be seen. The magnetic measurements were taken for one particular ramp-profile (the Tevatron collider run I ramp). The snapback duration in the Tevatron today is 6 sec because of a slower ramp. Figure 28 in appendix 5 shows the difference between the 96 and 02 current ramp profiles during the snapback. Chapter 7 will discuss further possible issues related to the snapback duration.
Comparisons such as in Figure 2 were also performed for other cases. Some plots are shown in appendix 2 (Figure 18 and Figure 19). Note that there is disagreement at the 0.2 unit level even at longer times in some cases. This should not alarm, however, given that the Tevatron b_2 fit represents the average of all Tevatron dipoles rather than the particular two magnets discussed here. Also, as will be discussed in chapter 4, the differences reflect beam based adjustments of the fit that were implemented during initial tune-up of the correction algorithm in the Tevatron.

4) Comparison of Decay & Snapback Fit and Magnet Data – Part II

The algorithm currently used for the b_2-decay and snapback correction is described in detail in chapter 2 (and was recently documented thoroughly in [4]). The following

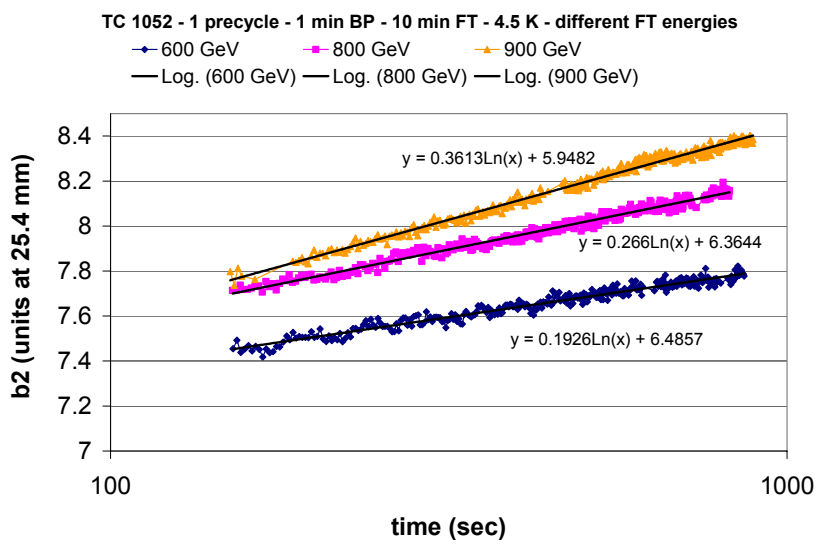

Figure 5: Example of fitting procedure for TC1052 b_2 decay data. The data shown represent cases with varying flat-top current in the pre-cycle. The flat-top condition is indicated in terms of the beam energy. The flat-top duration was 10 min, the back-porch time 1 min. The graph shows the b_2 as a function of time on the injection porch (as explained in the text the first 150 sec were removed from the data prior to fitting).

presents a new analysis of the 1996 magnetic measurements performed on the Tevatron dipole model TC1052. The original data analysis, which led to the algorithm presented in chapter 2, was published in [3]. The aim of this exercise is to determine how far the currently used algorithm has evolved from the initial parametrization. It is believed that this discrepancy is somehow indicative of the difference between the average Tevatron dipole magnet and TC1052. The following presents the recently obtained fits to the TC1052 data. These are the same data discussed partly in chapter 3.

The chosen fitting procedure consisted in using a least-square method to obtain the parameters, b_0 (intercept) and m (slope), of the function $b_0+m\ln(t)$ that fits best the decay data in the range 150 sec-15 min. The chosen time-interval is somewhat arbitrary, but reflects the fact that the TC1052 data indicate the existence of two time-constants in the logarithmic function, of which only the longer one is of interest here. Also, the b_2 at 1 sec was subtracted from the intercept (the additive constant in the logarithmic fit) to eliminate the geometric and hysteretic sextupole, which are not of interest for the drift and snapback fits. Figure 5 shows an example of the fitting procedure. The slope and intercept parameters were read directly from the trend-lines in the plot. Figure 21 and Figure 20 in appendix 3 show the slopes and intercepts found from the fits for cases of varying flat-top and back-porch times. Table 2 and Table 3 summarize the slopes and intercepts extracted from the fits of the decays for different back-porch and flat-top times. The so found intercept and slopes can be parameterized in terms of t_{bp} and t_{ft} such as in (2) and (3). This was done using a minimization algorithm in PAW. The obtained constants A-E are listed in Table 4. The discrepancy is small in B-E, but large in A. This results in a more negative b_2 intercept in the 96 data than what is currently used in the Tevatron fit. Although this is not immediately apparent from the data in Table 4, the discrepancy between the current fit ((2)-(3)) and the TC1052 data is most pronounced for

small flat-top times (which are rare conditions in the Tevatron). Figure 6 and Figure 22 (in appendix 3) show to which extent the TC1052 data and the current Tevatron fit agree. As mentioned above the discrepancy would increase if the magnet data would be corrected for the difference in flat-top energy between 96 (900 GeV) and today (980

Table 2: Slope data for TC1052 (4.5 K, 1 pre-cycle, 900 GeV flat-top) for different back-porch, t_{ext}, and flat-top, t_{ft}, times (in minutes).

t_{ft}(min) → t_{ext} (min) ↓	2	5	10	30	60
1	0.261	0.297	-	-	0.354
10	0.2	0.2	0.21	0.224	0.233

Table 3: Intercept (in units at 25.4 mm) data for TC1052 (4.5 K, 1 pre-cycle, 900 GeV flat-top) for different back-porch, t_{ext}, and flat-top, t_{ft}, times (in minutes).

t_{ft}(min) → t_{ext} (min) ↓	2	5	10	30	60
1	-0.98	-1.039	-	-	-1.276
10	-0.725	-0.722	-0.769	-0.833	-0.875

Table 4: Parameters of sextupole decay algorithm (2) and (3) as currently used in the Tevatron and as derived from the 96 measurement on TC1052 with PAW.

Parameter	A	B	C	D	E
As used today	0.04	0.161	0.0277	0.342	0.0208
Fit to TC1052 data	0.206	0.172	0.0539	0.456	0.019

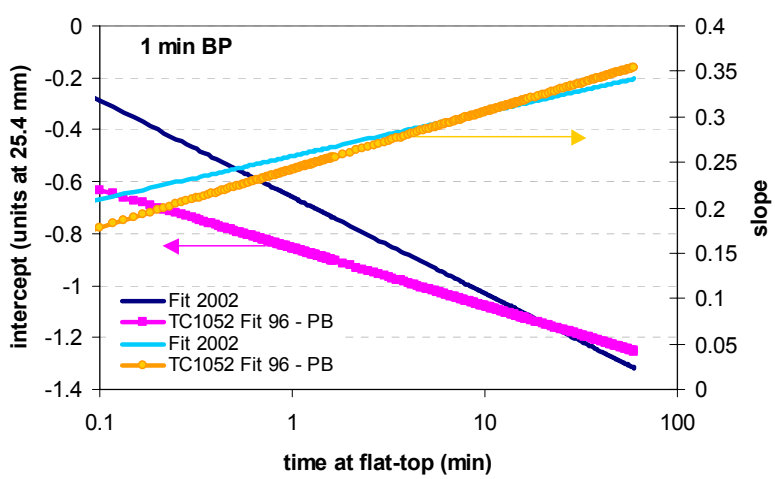

Figure 6: Comparison of slope and intercepts of current Tevatron decay fit and the latest fit to the 96 measurements in TC1052 for different flat-top times. The back-porch time is fixed at 1 min. The measurement conditions were: 1 pre-cycle, 900 GeV flat-top, 4.5 K.

GeV). Appendix 3 shows the fit to the measurements taken at varying flat-top energies (Figure 23). The discrepancy, most likely, reflects the fact that the average dipole magnet in the Tevatron has a behavior more closely described with the current fit than with A-E such as computed for the 96 data. Most of the parameter changes were implemented during the initial stages of the implementation of the fit in the Tevatron collider run II.

5) Beam Based B2 Measurements in the Tevatron

The preceding chapters discussed the b_2 decay and snapback correction schemes on the basis of measurements performed on magnets. This chapter discusses recent measurements of b_2 using beam based chromaticity measurements. Beam chromaticity measurements have been performed many times before during the injection porch in order to verify the Tevatron b_2 compensation scheme. A measurement of the chromaticity during the injection porch performed by B. Hanna on Aug. 18th 2001, for example, (30 min dry-squeeze, 1 min back-porch) revealed a chromaticity of 1-2 units within the set-point (or 0.2 units of b_2, taking into account that 1 unit of uncompensated sextupole in the 774 Tevatron dipoles results in ~25 units of horizontal chromaticity). This indicates that the sextupole during the drift is controlled to the level of 0.1 units, which is reasonably good.

The following will describe beam based chromaticity measurements taken recently, not only during the injection porch, but also during the ramp. The beam-based b_2 derivation uses measurements of the chromaticity to derive the b_2 in the magnets. The derivation of the magnet b_2 from the beam chromaticity assumes that the measured chromaticity is given as the sum of the natural chromaticity (ξ_{nat}), the b_2 in the dipole magnets (ξ_{b2mag}) and the (compensating) b_2 supplied by the sextupole correctors (ξ_{b2corr}) (see equation 7). Knowing the natural chromaticity from lattice simulations (such as using a Tevatron lattice model in MAD) as well as the b_2 supplied by the sextupole correctors (derived from the sextupole correction currents extracted from the Tevatron control program together with equations (5), (6) and (9) from the appendix 1), the magnet b_2 can be derived on the basis of the measured chromaticity. The chromaticity related to the magnet b_2 can then be converted to the b_2 with equation 9b (see appendix 1 for details).

$$\xi_{tot} = \xi_{nat} + \xi_{b2mag} + \xi_{b2corr} \tag{7}$$

Measurements of the Tevatron beam chromaticity were performed twice recently in order to check the Tevatron b_2 compensation scheme. These measurements are described in detail in [6]. The chromaticity measurements were performed with an un-coalesced protons-only beam on the center orbit (helix off). The Tevatron was prepared with a pre-cycle (20 min dry squeeze) such as for a regular shot. After injecting an un-coalesced proton beam the tunes were measured as a function of time during the injection porch as well as up the ramp. This measurement (including the beam-less pre-cycle) was performed for different RF frequency settings (-20, 0, +20 Hz). The derivative of the tunes as a function of RF frequency gives the instantaneous chromaticity. The chromaticity was calculated for all the times during the injection porch and up the ramp.

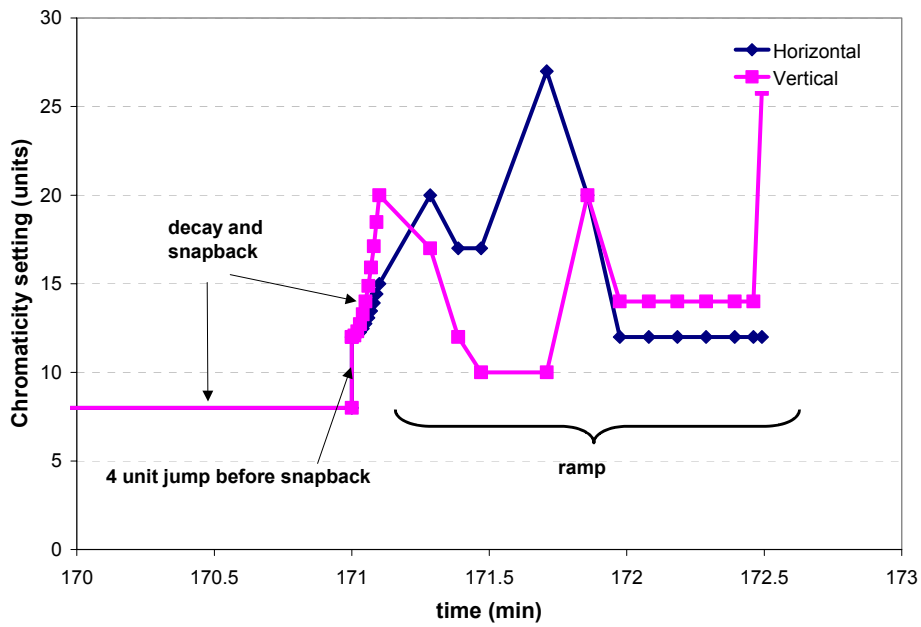

Figure 7: Tevatron chromaticity measured during Sept. 18th 2002 run.

An example of the result of such a measurement is shown in Figure 7. Figure 8 and Figure 9 show the b_2 derived from the chromaticity measurements in the Tevatron. The magnet b_2 was inferred from the magnet contribution to the chromaticity, ξ_{b2mag}, using (7), (5), (6) and (9b - see appendix 1). The curves shown in fact represent the average computed from the b_2 derived from the vertical and horizontal chromaticities. The agreement between the derivations based on the measurements of the vertical and horizontal tunes is within ~0.2 magnetic units of b_2. Figure 8 shows a measurement during the injection porch together with a set of magnet (TC0504) data from the 96 measurements. The drift is shown as a function of time for better representation. The agreement between magnet data and the b_2's derived from the correction currents is fair. Note that the magnet b_2 data were offset corrected to fit the beam based data. The offset correction procedure consists in subtracting the geometric sextupole of TC0504 (12.4 units) and adding a b_2 of 0.8 units. Essentially the offset correction transforms TC0504 into the average Tevatron magnet (see chapter 6 for more details on this procedure). Also note that the injection porch in the magnetic measurement lasted only 15 min vs. more than 171 min in the beam based measurement. Figure 9 shows the three beam based b_2 measurement over the entire ramp. The third case consists only of a measurement at flat-top [9]. The other two measurements also comprise the snapback.

The snapback is different in both cases because of the difference in injection porch duration. The smaller snapback occurs for the 20 min injection dwell, the larger after a 171 min dwell on injection.

The measurements show that the b_2 derivation on the basis of beam chromaticity measurements appears to have a precision of the order of 0.5 units, which is approximately the difference between the three data sets during the ramp. It is unlikely that the magnet conditions during these three runs were the cause of that difference. The average magnet temperature, for example, would have to be different by ~1 K to explain

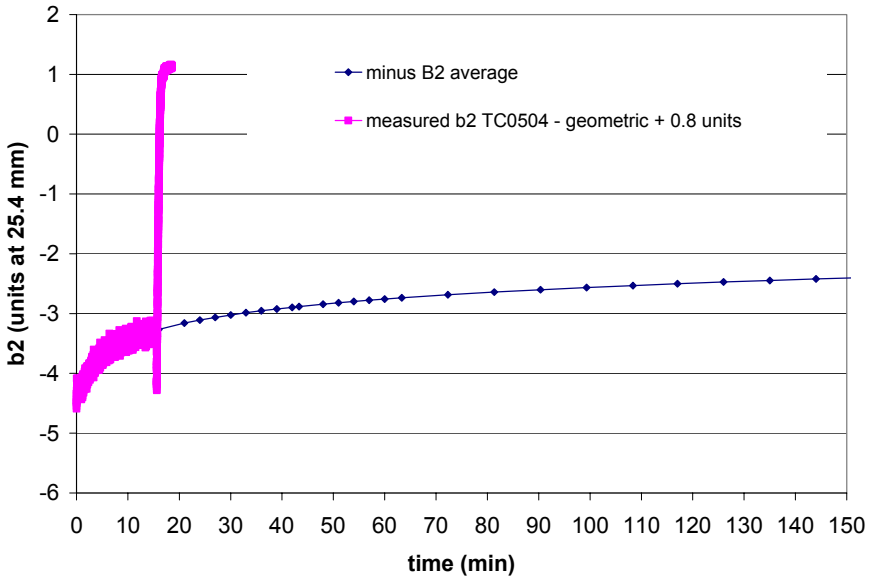

Figure 8: Sextupole as measured in TC0504 (without geometric sextupole) on Sept. 18th 2002 compared to b_2 derived from compensation currents in Tevatron control system.

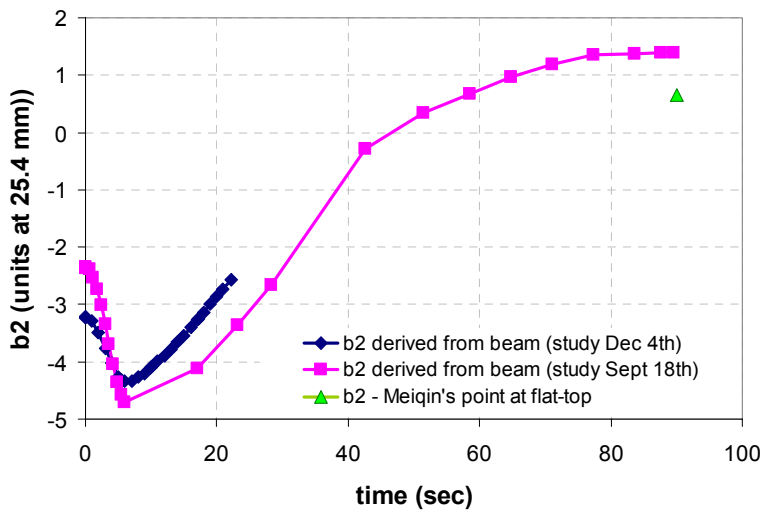

Figure 9: Beam based measurements of b_2 in the Tevatron, data are from [6,9].

this magnitude. Unfortunately 0.5 units of uncertainty is too large to allow drawing significant conclusions on the basis of beam based measurements alone. However, in combination with magnet measurements, as shown next, some more confidence can be gained in the data and their interpretation.

6) Comparison of Beam and Magnet Based B2 Measurements

The beam-based b_2 measurements up the ramp discussed in chapter 5 need to be compared to the b_2 measured on magnets in order to allow judgment of the quality of the b_2 compensation scheme in the Tevatron. The magnetic measurement data recorded in 96 on TC1052 and TC0504, together with recent measurements on three magnets (TC 1220, TC0483, TB0834), allow for such a comparison. It is important to point out that a single magnet does not necessarily have the same b_2 characteristics as the average magnet, inferred from beam based chromaticity measurements. The explanation for this discrepancy lies within the magnet-to-magnet differences in geometric and hysteretic (as well as dynamic) b_2. Reference [2] discusses the fact that the average geometric b_2 in the Tevatron, derived from the magnetic measurement archive data, must be 1.47 units. The geometric b_2 obtained in the magnetic measurements of the magnets listed above (see for example Figure 1) does certainly not agree with this number, not only because of the magnet-to-magnet spread in b_2 characteristics, but because the measurements were taken with rotating coil probes inserted far into the magnet, such as to measure the body fields only. As discussed in detail in [2] there is a strong difference in b_2 in the ends and body of the Tevatron dipoles and only the body-end-average is close to zero. Then, the width of the hysteretic curves measured on all Tevatron dipoles during production, shows a spread of ~±1 unit at 150 GeV that can lead to a strong mismatch between a single magnet hysteretic b_2 measurement and the average b_2 derived from beam-based measurements. Figure 24 - Figure 27 in appendix 4 show histograms produced from the Tevatron dipole magnetic measurement data archive. The average b_2 characteristics derived from these histograms are summarized in Table 5. They allow the archive data based reconstruction of the geometric and hysteretic b_2 behavior of Tevatron dipoles discussed here.

Table 5: Geometric and hysteretic b_2 characteristics of all Tevatron dipoles installed, as derived from the magnetic measurement data-base. Measurements that suffered current overshoots were removed from the width data (see brief discussion in appendix 4).

	geometric	width @ 660 A	width @ 2 kA	hysteretic at 4 kA
average	1.47	9.9	1.5	0.83
sigma	3.09	0.82	0.27	3.04

The hysteretic b_2 loop of the average dipole installed in Tevatron can be approximately reconstructed from the 660 A, 2 kA and 4 kA points. It is hoped that the beam based measurements agree well with the so found average b_2 loop, since this is what the beam based b_2 measurement is supposed to represent. There is, however, an issue, which should result in a discrepancy in the two data sets. This issue is the fact that the production magnetic measurements in the early 1980s were performed at constant current. Thus the current ramp was stopped at the measurement points (660 A, 2 kA, 4 kA) and the data-points taken. During this current plateau the b_2 was drifting, a fact that was unknown at that time. Therefore the archive data include an unknown amount of drift in the multipoles. This drift occurs toward the geometric and therefore results in an

underestimation of the width of the hysteretic loops. This under-estimation in width can easily be as much as 2×0.5 units of sextupole.

Figure 10 and Figure 11 show the results of magnetic and beam based b_2 measurements combined. Figure 10 shows the combined data as a function of time. Only three magnetic measurement results (from TC1220, TC0483, TB0834) are included because the 96 data were recorded on a different ramp-profile (the Tevatron collider run I ramp). The magnetic measurement data were converted to 4 K, if necessary. 4 K is believed to be close to the average temperature in all of the Tevatron dipoles [8]. The temperature conversion consisted in scaling the entire loop with a factor 1.13 per K temperature difference between the temperature of the actual magnetic measurement (typically 4.5 K) and the estimated average Tevatron dipole temperature of 4 K. Besides the two beam-based measurements the plot also contains the reconstructed average hysteretic loop using the archive data from Table 5. The error-bars (strictly speaking they are not error bars) added to the points of the reconstructed hysteresis represent the standard deviation of the hysteresis width distribution measured on the entire magnet population. Therefore

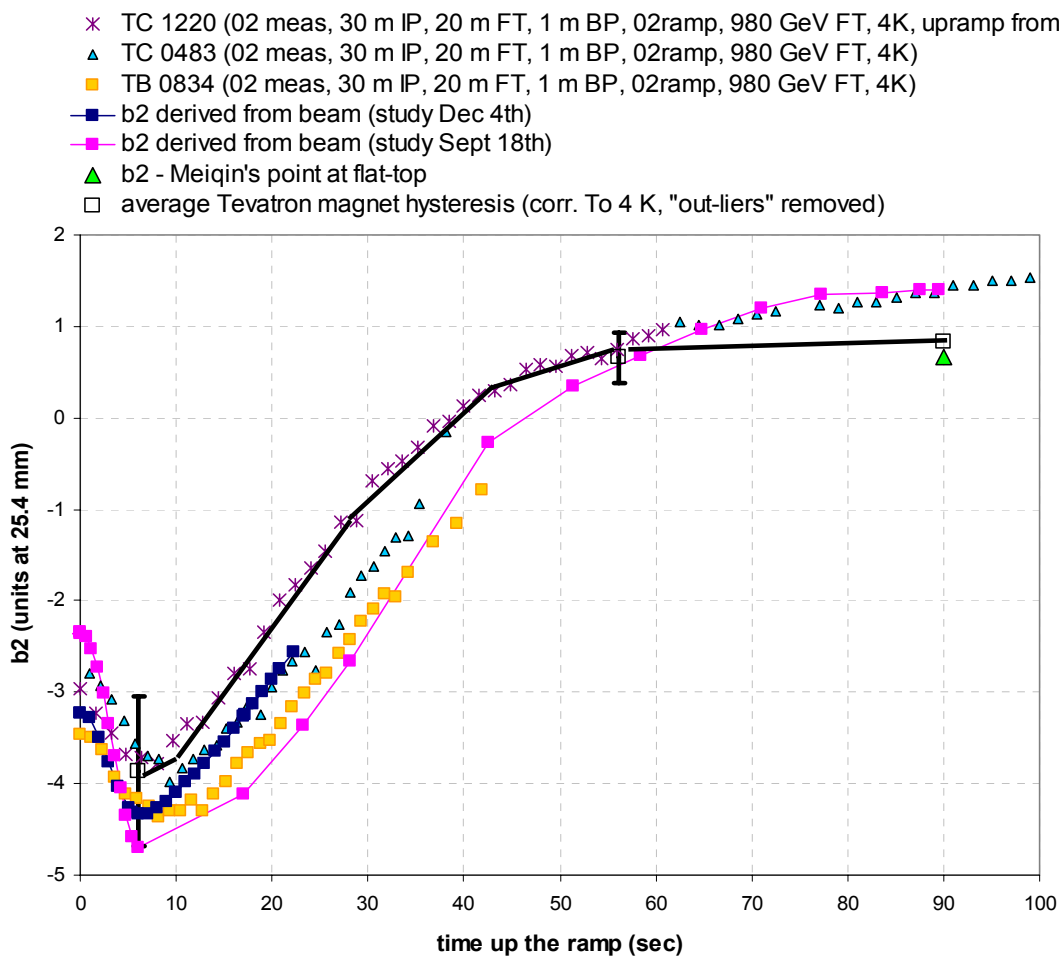

Figure 10: Comparison of beam- and magnet-based b_2 measurements. Hysteretic loops of magnetic measurements were converted to 4 K, if necessary. Also, all magnetic measurements were moved into the average Tevatron dipole geometric of 1.47 units. The beam-based data are from [6,9].

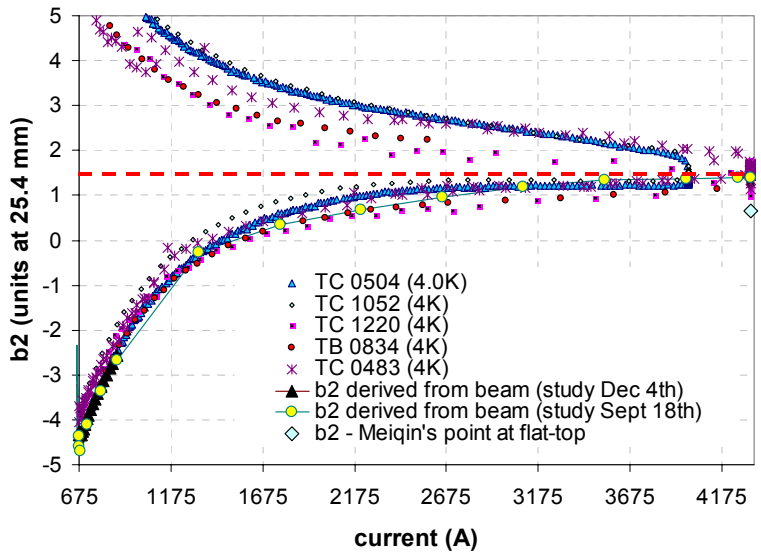

Figure 11: Comparison of beam- and magnet-based b_2 measurements. Hysteretic loops of magnetic measurements were converted to 4 K if necessary. Also, all magnetic measurements (which were obtained in the magnet body and therefore reflected the typical ~14 units of geometric body b_2) were moved into the average Tevatron dipole geometric of 1.47 units (red dashed line). The beam-based data are from [6].

the hysteretic loops measured on particular magnets can lie anywhere within (or also outside) the range delimited by the brackets. The three magnets shown are indeed comfortably within this $\pm 1\sigma$ bracket. The uncertainty of the beam-based b_2 measurement was discussed in chapter 5. Single magnet measurements are precise to less than 0.1 (magnetic) units. The discrepancy between the beam based measurement and the re-constructed average Tevatron dipole b_2 is therefore related either to the inaccuracy of the beam-based measurement, or, even more likely the result of drift that occurred during the production magnetic measurements (as discussed above). The better agreement between the reconstructed hysteresis and the beam based measurement could be a hint toward this effect. Note that also the reconstructed hysteresis has been scaled to 4 K (from the standard measurement temperature of 4.6 K). Figure 11 shows the beam-based and some magnet-based b_2 measurements combined as a function of current. In this case the magnetic measurements from 1996 (TC1052 and TC0504) could be included! The plot shows a satisfactory agreement between beam based data and magnet measurements. Note, however, that the agreement at the single magnet level is not expected, given the wide spread in hysteretic loop width (and shape) observed in the population of Tevatron dipole magnets.

7) Conclusions

We have found that the current Tevatron b_2 decay and snapback correction is within ~0.2 units of the b_2 measured in dipole model TC1052, the degree of discrepancy depending on the pre-cycle conditions (range analyzed: flat-top time between 2-60 min, back-porch

time 1-10 min). The discrepancy is not surprising since it merely reflects the fact that TC1052 is not exactly like the average Tevatron dipole, rather its b_2 is within 0.2 units of the average. That the currently used fit is representative of the average magnet is furthermore confirmed by the fact that sporadic chromaticity measurements during injection also indicate that the b_2 is controlled to within 0.1 units.
Beam based chromaticity measurements allow for an approximate derivation of the average dipole b_2 in the Tevatron. Such measurements were performed and data on the average magnet b_2 during drift, snapback and ramp to collision were derived. These data were compared to the geometric, hysteretic and dynamic b_2 measured on magnets in 96, [3], and recently, [7], as well as a theoretical average magnet reconstructed from the magnetic measurement archive data taken during magnet production. This comparison revealed a fair agreement between beam-based and magnet-based b_2 measurements, but suffers from a lack of precision in the derivation of b_2 from beam chromaticity as well as the magnet-to-magnet spread in essentially all b_2 characteristics (but most importantly the unknown spread in terms of their dynamic properties which are not known in the case of the majority of the Tevatron dipoles).
The extensive analysis conducted here, however, allows us to conclude, within the constraints of our measurement accuracy, that the b_2 correction scheme in the Tevatron is successfully compensating for the geometric, hysteretic and dynamic b_2 effects in the Tevatron dipole population.
There are five issues that have been discussed in detail recently in the context of new measurements on additional spare Tevatron dipoles, reported in [7]. Some of these issues were resolved. Others could be resolved in the future with minor improvements of the drift and snapback compensation algorithm, as defined in equations (1)-(4).

-1- The b_2 value at injection (150 GeV) is a well defined value, that should not depend on powering history, nor on ramp-rate (at least within a range of ramp-rates typical of the Tevatron's ~50 A/s). Magnetic measurements performed in 96 as well as today show a variation of this value, referred to as intercept in the b_2 algorithm (equation 2), that is beyond the typical noise of rotating coil measurements. Figure 12 shows the spread of the b_2 at injection (before the start of the drift) measured recently on TC0269. A variation of the order of ±0.1 units was seen. The cause of this variation is now believed to be related to the longitudinal field patterns caused by the current imbalances that are at the root of the dynamic magnetic effects. This sinusoidal field variation typically has a periodicity given by the cable twist pitch, which is ~2.5 inches in the Tevatron dipoles. If the length of the rotating coil probes, with which the magnetic measurements are made, is not an integer multiple of the period of the pattern, powering history dependent effects are to be expected, since the amplitude of the pattern depends on the powering history. We therefore believe that the history dependence of b_{2ini} is an artifact of the magnetic measurements probes not being an integer number of periods of the periodic field pattern. Therefore a variation of b_{2ini} with pre-cycle parameters should not be implemented in the Tevatron chromaticity correction, such as it is currently done (equation 2). Note that the beam definitely integrates over the longitudinal pattern. It has to be noted, however, that the parameter b_{2ini}'s main purpose is to off-set the correction algorithm by ~-1 unit, such as to allow a fit of the magnet b_2 at larger times with a one-time constant logarithmic function. The history part of the b_{2ini} fit represents only a variation at the 0.1 unit level.

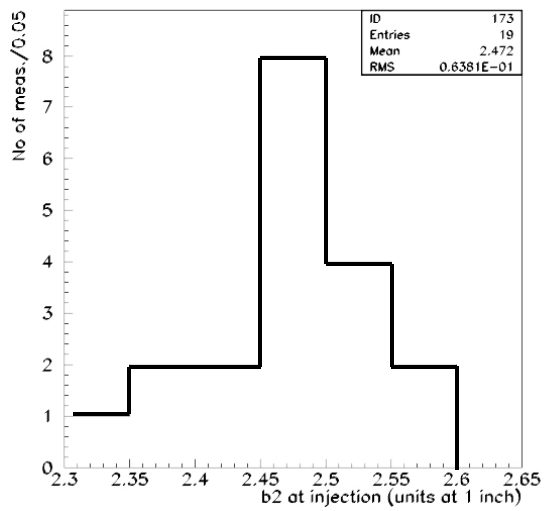

Figure 12: Histogram of b_2 at injection (150 GeV) recorded in 19 measurements on TC0269, [7]. The noise level in these measurements was ~0.1 units at 25.4 mm.

The correction suggested here, will therefore change the Tevatron b_2 correction by very little, ~0.1 units or so.

-2- The Tevatron b_2 snapback fit uses a 4th order polynomial (with only even terms) as a function of a single parameter, the snapback time (equation 4). All snapback measurements performed in 1988, 1992 and 1996 reveal a snapback shape that is suggestive of the polynomial function. We would like to point out, however, that the snapback is slightly altered after removing the hysteretic b_2 growth (between 150 and ~153 GeV) occurring during the snapback. The fact that the baseline is changing during the snapback was not taken into account in former magnet measurement data analysis (because it is small, of the order of 0.1-0.2 units). It should be taken into account since the base-line change is in principle already corrected for in the sextupole corrector protocol that addresses the hysteretic b_2 evolution. Figure 14 shows that, after subtraction of the hysteretic baseline, such as in the particular example shown (magnet TC0269, measurement reported in [7]) an exponential fit is better. The exponential fit, besides fitting data better, is also more in tune with the physics model of the process (briefly discussed in chapter 1) and it is more robust. The greater robustness is given by a smaller sensitivity of the time constant, τ, to data noise at the end of the snapback. A possible implementation of the exponential snapback fit is given in (8).

$$b_2^{snap}\left(t_{ext}, t_{ft}, t_{inj}, t\right) = b_2\left(t_{ext}, t_{ft}, t_{inj}\right) e^{-\frac{t}{\tau\left(t_{ext}, t_{ft}, t_{inj}\right)}} \quad units\ at\ 25.4\ mm \tag{8}$$

The disadvantage of the exponential fit, as can be seen from equation (8), is that the exponential time constant τ depends on the history parameters through the drift amplitude. This is a result of the fact that the snapback takes a more or less fixed amount

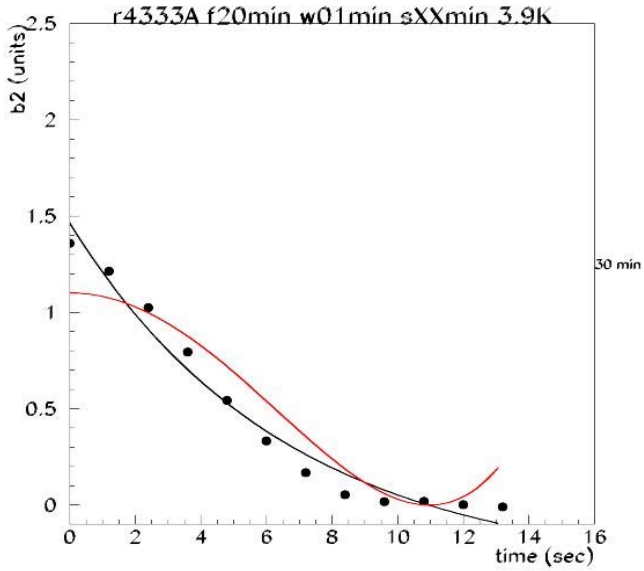

Figure 13: Polynomial and exponential fits of a snapback measured in TC0269 after a 30 min drift following a standard Tevatron pre-cycle (20 min flat-top, 1 min back-porch).

of time, such that after a longer drift (and increased drift amplitude) the snapback time constant needs to be smaller.

-3- A related issue is that the snapback duration appears to be more or less independent of powering history. The beam based b_2 measurements reported in [6] and shown in Figure 15 show that this also holds true in the Tevatron. Magnetic measurements show that there is a correlation between drift amplitude and snapback current, that is the current (or field or beam energy) it takes for the snapback to be completed. This is consistent with the physics model briefly introduced in chapter 1, since larger drift is the result of a larger local field change due to current redistribution and therefore more main field is required to overcome the local field change and bring the b_2 back to the hysteretic loop. The reason for the Tevatron not showing a longer snapback time after a longer drift could be that the b_2 drift saturates after a certain time. All magnet measurements performed so far (on ~10 magnets, [4]) and beam-based measurements in the Tevatron, [6, and see Figure 15], indicate that this does not occur, i.e. the longer the dwell at injection porch the larger the drift amplitude usually is. The reason, in fact, for the (near) constancy of the snapback duration most likely is the parabolic ramp profile (see Figure 28 in appendix 5) in the Tevatron. Figure 14 shows two plots representing the snapback in TC0269 after 30 , 60 and 120 min on injection porch. One plot shows the snapback as a function of time, the other as a function of current. Indeed the snapbacks, although starting from different drift amplitudes, occur within approximately the same time. The right plot, however, clearly shows that the snapback is completed within 22 A, 23 A and 29 A after drifting to 1.5, 1.6 and 1.9 units, giving more or less the expected 1:1 correlation. The one-time-fits-it-all approach appears to introduce an operational inaccuracy of the order of 0.2 units (as judged from the discrepancy between fit and beam based data shown in

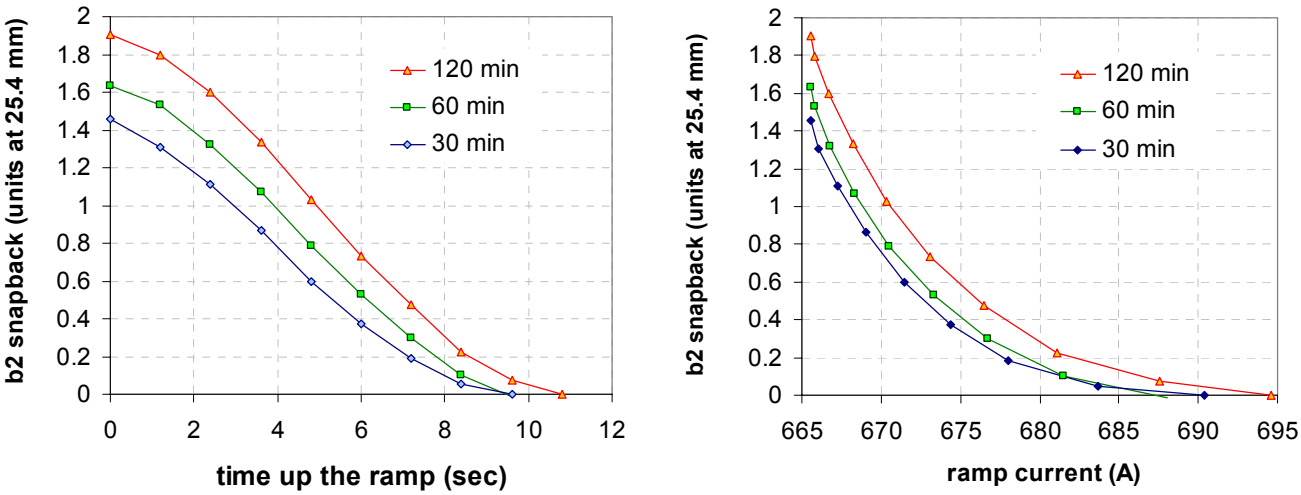

Figure 14: b_2 snapback in TC0269 after a 30, 60 and 120 min injection porch following a standard Tevatron pre-cycle (20 min flat-top, 1 min back-porch). Left: snapback as function of time; Right: snapback as function of current;

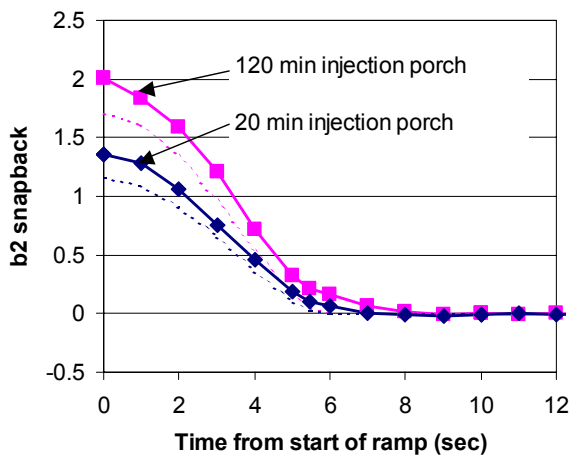

Figure 15: Beam based derived b_2 snapback after a 20 min and a 120 min injection dwell. Also shown are the Tevatron snapback fits. The data are baseline corrected (the growth of hysteretic b_2 during the snapback was subtracted).

Figure 15. The correction of this operational inaccuracy would go hand in hand with the introduction of an exponential fit.

-4- Figure 16 shows the effect of the following inaccuracy in Tevatron operations on the b_2 drift and snapback fit. At the end of the back-porch dwell (now typically 1 min), the T:CHROM module is loaded to calculate (among other things) the parameters of the drift and snapback fit during the subsequent injection porch. This operation takes typically 20 secs during which the Tevatron is waiting at the back-porch. Therefore the real back-porch time is ~83 sec, rather than the ~60 secs that T:CHROM used in the algorithm to

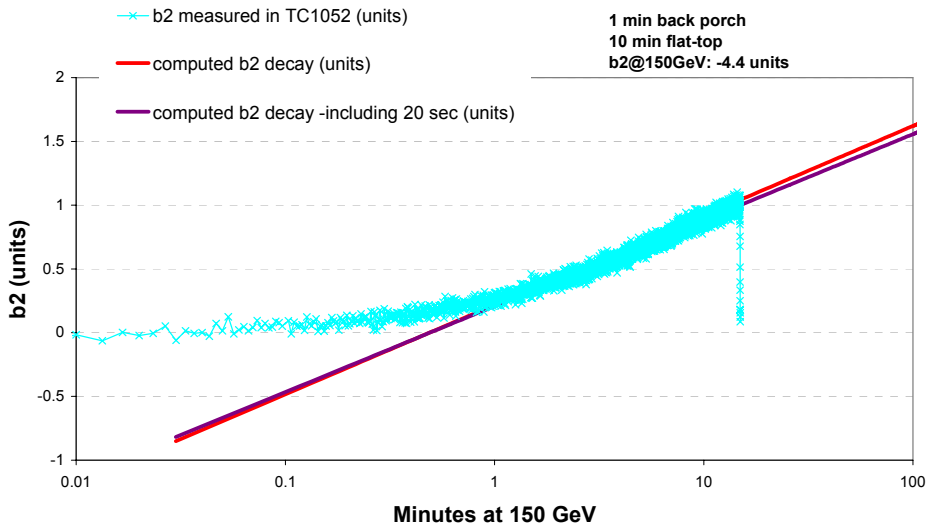

Figure 16: Drift corrections for a 60 and 80 sec back-porch compared to the magnetic measurement on TC1052.

prepare the following injection porch. Figure 16 shows that the prolonged stay of ~20 sec at the back-porch induces an error in the fit parameters of the order of 0.1 units.

-5- As a conclusion of this discussion we are adding recently acquired data of snapbacks in four Tevatron dipoles (Figure 17) following a standard Tevatron pre-cycle (20 min dry-squeeze, 1 min back-porch). In the case of magnet TC0269 two measurement methods are compared, rotating coils and a Hall-probe-sensor array, recently provided by Cern in the frame of a collaboration on magnetic measurements [10]. The data are also compared to the beam-based data discussed in chapter 5 and the fit (equ 4) currently used in the Tevatron. Table 6 lists the drift amplitude and snapback duration measured in these four magnets as compared to the Tevatron fit. The plot and the table clearly reflect the issues at hand. There is a large spread in the dynamic b_2 properties (such as the drift amplitude) among Tevatron magnets, most likely related to magnet-to-magnet variations in inter-strand contact resistances within the
magnet cables as well as superconductor properties (such as for example critical current density). The average dynamic b_2 properties of the ensemble of dipole magnets installed in the ring are not known because they were never measured. Despite this caveat, we believe that enough data have been gathered in this recent study to come to the conclusion that the Tevatron b_2 compensation works properly to a level of ~0.1 b_2 units. Only a few minor inaccuracies (discussed above) could be detected, thanks to an improved understanding of dynamic effects in superconducting magnets today. We suggest that these issues should be resolved in the near future.

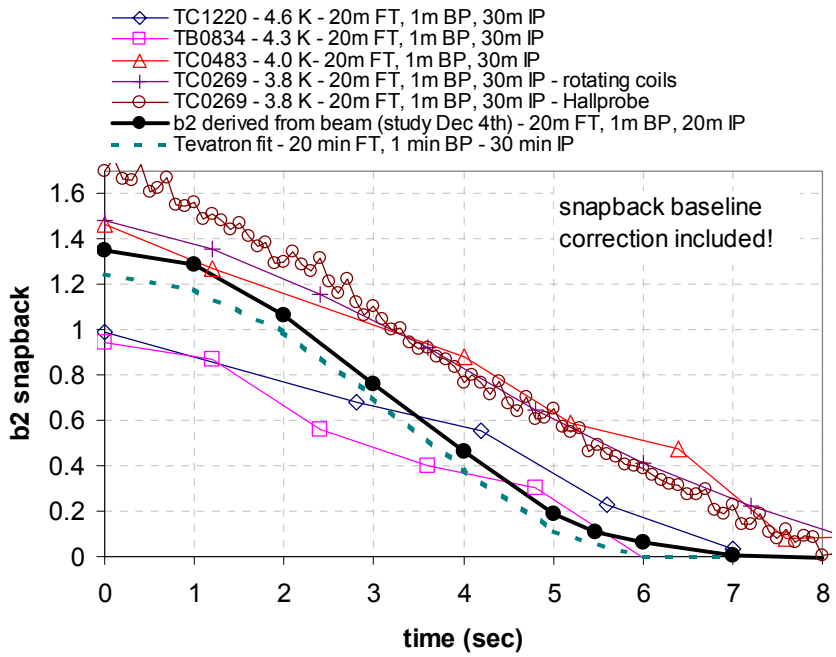

Figure 17: Comparison of snapbacks measured on four Tevatron dipole magnets after a 30 min drift following a 980 GeV - 20 min flat-top - 1 min back-porch pre-cycle with the fit currently used in the Tevatron for similar conditions. In addition a beam-based measurement after a 20 min drift is shown (see [6]). In the case of magnet TC0269 the results obtained with two different measurement techniques are given. All snapbacks were base-line corrected (the growth of hysteretic b_2 during the snapback was subtracted). The data shown in the plot are also reported in Table 6.

Table 6: Summary of drift amplitude and snapback duration measurements on four Tevatron dipoles (reported in [6]) as compared to the current Tevatron b_2 compensation fit. The magnet data were taken following a standard Tevatron pre-cycle (20 min flat-top, 1 min back-porch). The data were not corrected for temperature differences. The reported b_2 was measured at the 25.4 mm reference radius.

Magnet	TC1220	TC0834	TB0483	TC0269	Tevatron-fit
Drift after 30 min (units)	0.99	0.85	1.5	1.58	1.25
Snapback duration (sec)	6.6	6.5	9	8.2	6
Temperature (K)	4.5	4	4	3.8	~4[8]

APPENDIX 1

The units of sextupole, b_2, can be converted to current in the two sextupole circuits (T:SFB2 and T:SDB2) via the chromaticity relation (at 150 GeV):

$$\begin{pmatrix} \Delta\zeta_x \\ \Delta\zeta_y \end{pmatrix} = \begin{pmatrix} 45 & 8.9 \\ -14.36 & -26.96 \end{pmatrix} \begin{pmatrix} I_{T:SF} \\ I_{T:SD} \end{pmatrix} \qquad (units\ of\ chromaticity) \tag{9a}$$

and the relation between chromaticity and b_2 in the dipoles:

$$\begin{pmatrix} \Delta\xi_x \\ \Delta\xi_y \end{pmatrix} = \begin{pmatrix} +26.22 \\ -23.92 \end{pmatrix} b_2 \quad (units\ of\ chromaticity) \tag{9b}$$

The matrix elements $M_{i,j}$ in (9a) can be calculated from (10), where the index i stands for x,y and the index j for SF and SD. The lattice functions in both circuits are given in Table 7.

$$M_{i,j} = \frac{1}{4\pi} \times 88 \times \langle \beta_i D_i \rangle_j \frac{449\,T/m}{(500\,Tm)_{dip} \times 50A} = \frac{1}{4\pi} \times 88 \times \langle \beta_i D_i \rangle_j \times 0.01795 \left(\frac{units}{A} \right) \tag{10}$$

Table 7: Sextupole corrector characteristics (calculated with Tevatron lattice model in MAD).

Circuit	Number of elements	Average β_x (m)	Average β_y (m)	Average D_x (m)	Average β_x*D_x (m^2)	Average β_y*D_x (m^2)
T:SF	88	93.81	30.09	3.810	358.7	115.8
T:SD	88	30.30	93.29	2.301	70.84	214.6

The coefficients in (9b) can be calculated similarly (on the basis of MAD model data) from (11):

$$\xi_x = \frac{1}{4\pi} \sum \beta_x K_2 L D_x = \frac{1}{4\pi} N_{dip} \langle \beta_x D_x \rangle L_{dip} K_2 = \frac{1}{4\pi} N_{dip} \langle \beta_x D_x \rangle L_{dip} \frac{2B_0 b_2 10^{-4}}{B\rho r_0^2} =$$

$$= \frac{774 \cdot 170 \cdot 6.12 \cdot 2 \cdot 0.66 \cdot b_2 10^{-4}}{4\pi \cdot 500 \cdot (0.0254)^2} = 26.22 \cdot b_2$$

$$\xi_y = -23.92 \cdot b_2 \tag{11}$$

As can be seen in (11) the sextupole strength K_2 is defined as $(2B_0 b_2 10^{-4})/(B\rho r_0^2)$. Inverting the matrix in (9) and using (11) gives equation (12) for the currents in the correctors (at 150 GeV).

$$\begin{pmatrix} I_{T:SF} \\ I_{T:SD} \end{pmatrix} = \frac{1}{1085}\begin{pmatrix} -26.96 & -8.9 \\ 14.36 & 45 \end{pmatrix}\begin{pmatrix} +26.22 \\ -23.92 \end{pmatrix} b_2(units) \qquad (A) \tag{12}$$

Equation (12) can be written line by line to give the linear current-b_2 relations:

$$I_{T:SFB2}(t) = -0.454\, b_2(units) \quad (A) \tag{13}$$

$$I_{T:SDB2}(t) = -0.646\, b_2(units) \quad (A) \tag{14}$$

The constants quoted in (13) and (14) are the calculated values for the Tevatron. They do not match exactly those measured in the Tevatron (see equations (5) & (6) in the text). For further discussion consult reference [6].

APPENDIX 2

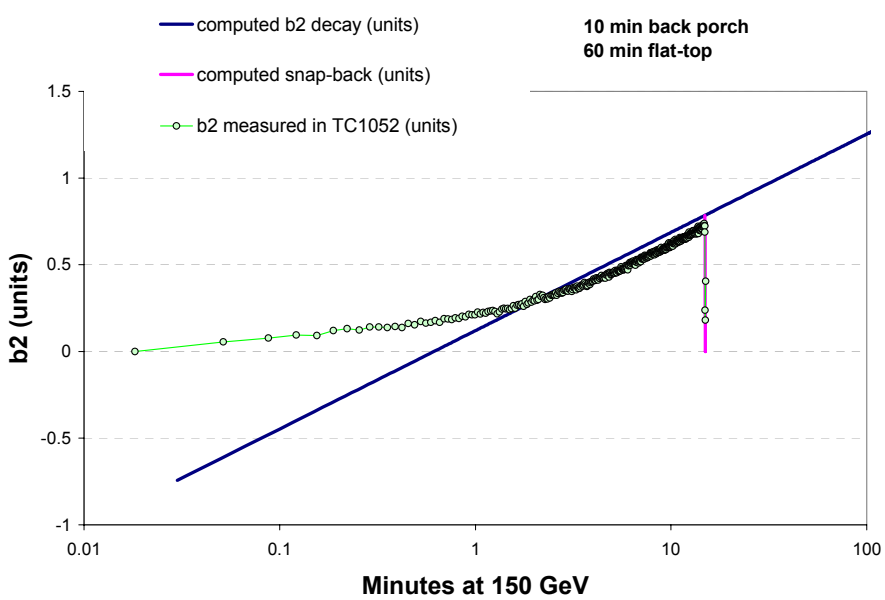

Figure 18: Sextupole decay in TC1052 for 10 min back-porch and 60 min flat-top conditions as compared to the calculated sextupole (equ (1)-(4). The b_2 is given in units at 25.4 mm.

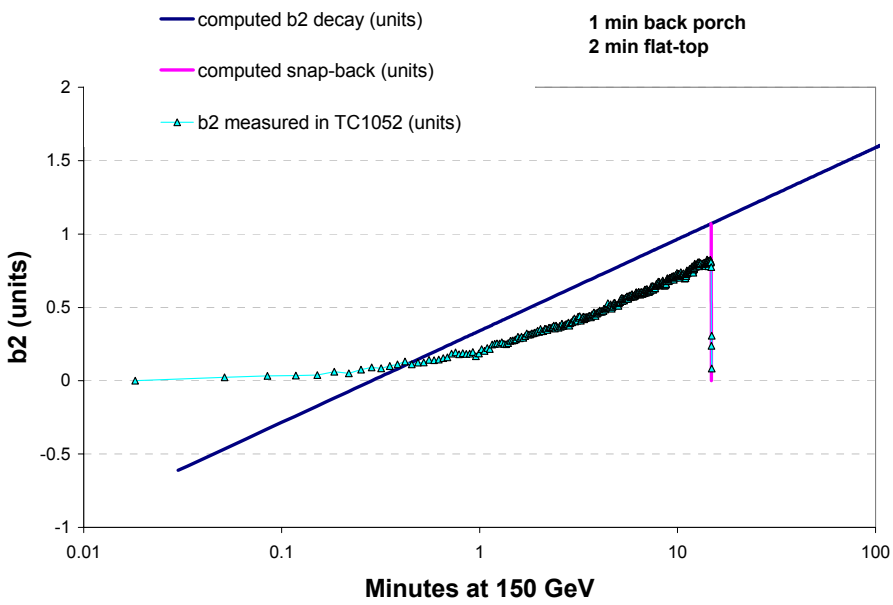

Figure 19: Sextupole decay in TC1052 for 1 min back-porch and 2 min flat-top conditions as compared to the calculated sextupole (equ (1)-(4). The b_2 is given in units at 25.4 mm.

APPENDIX 3

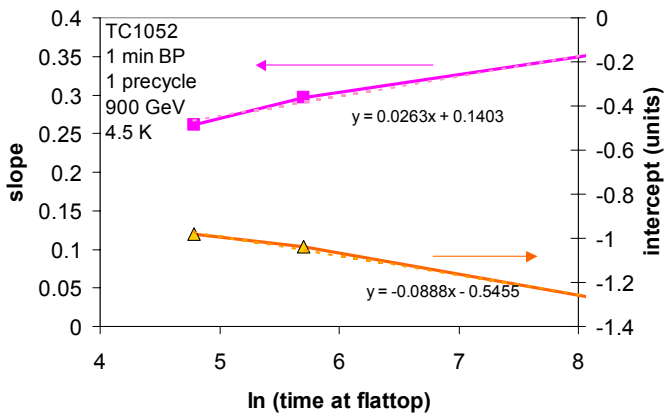

Figure 20: Slope and intercept (in units at 25.4 mm) parameterization in flat-top time (in seconds) of TC1052 data (back-porch time is 1 min).

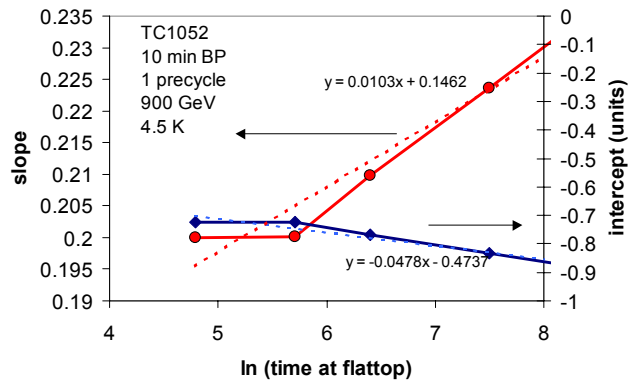

Figure 21: Slope and intercept (in units at 25.4 mm) parameterization in flat-top time (in seconds) of TC1052 data (back-porch time is 10 min).

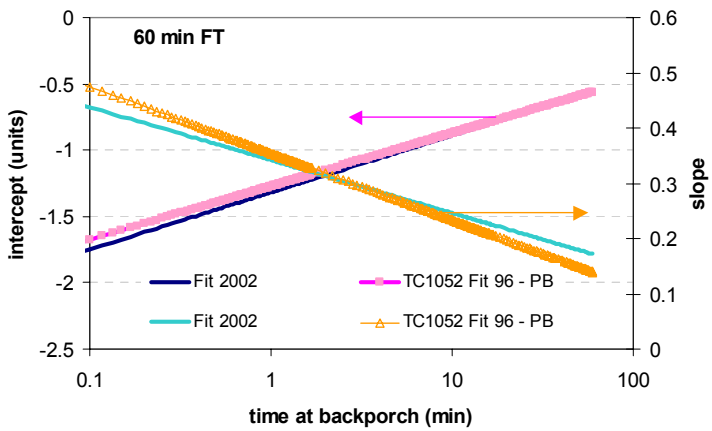

Figure 22: Comparison of slope and intercepts (in units at 25.4 mm) of current Tevatron decay fit and the latest fit to the 96 measurements in TC1052 for different back-porch times. The flat-top time is fixed at 60 min. The measurement conditions were: 1 pre-cycle, 900 GeV flat-top, 4.5 K.

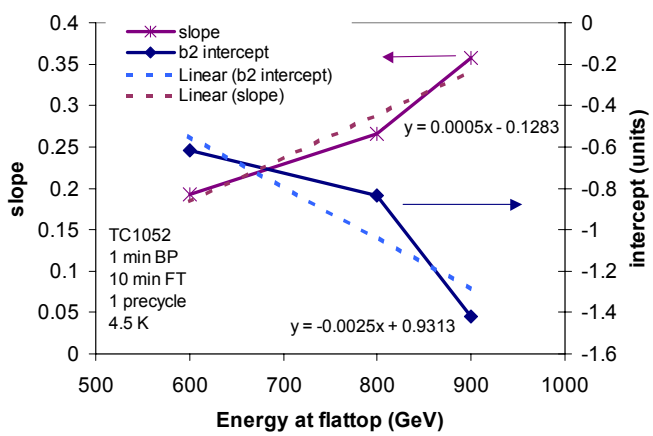

Figure 23: Slope and intercept (in units at 25.4 mm) parameters for TC1052 for a 10 min time at different flat-top energies. A linear fit of the data is shown as well. The measurement conditions were: 1 min back-porch, 1 pre-cycle, and 4.5 K.

APPENDIX 4

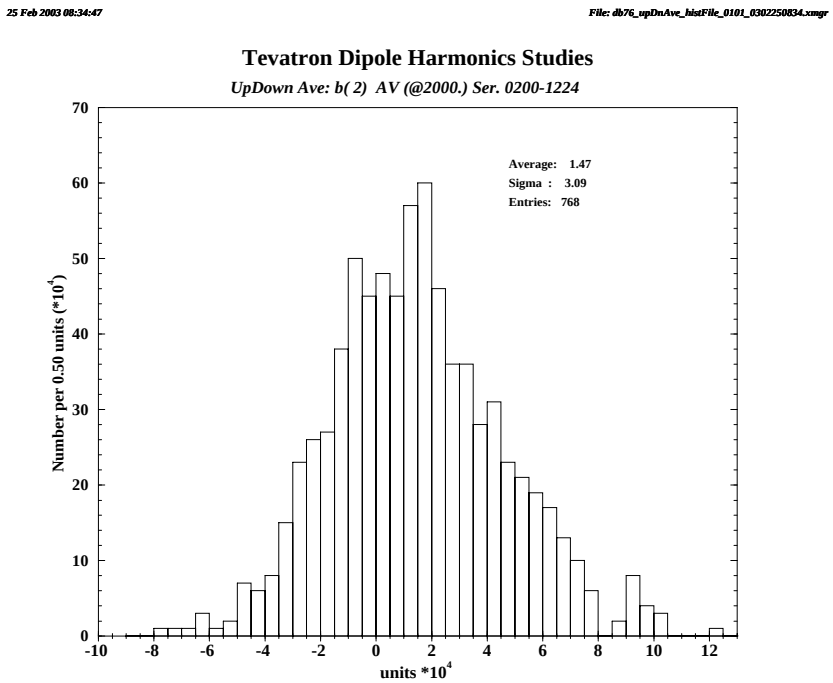

Figure 24: Tevatron dipole archival magnetic measurement data: Average geometric b_2 (in units at 25.4 mm) of all Tevatron dipoles installed, as calculated from the up-down average at 2000 A (up-down referring to the up and down branch of the hysteresis loop).

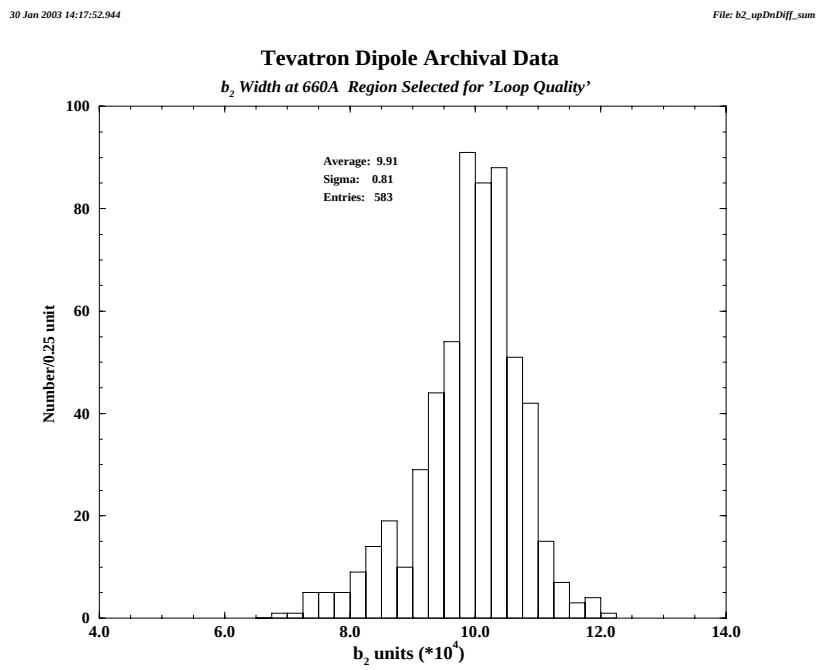

Figure 25: Tevatron dipole archival magnetic measurement data: Distribution of b_2 loop width (in units at 25.4 mm) at 660 A of all Tevatron dipoles installed. “Outliers”, that is data points indicating a narrower loop due to faulty measurements, were removed from the data-set. A known measurement fault leading to narrow loops is the current overshoot on the down ramp.

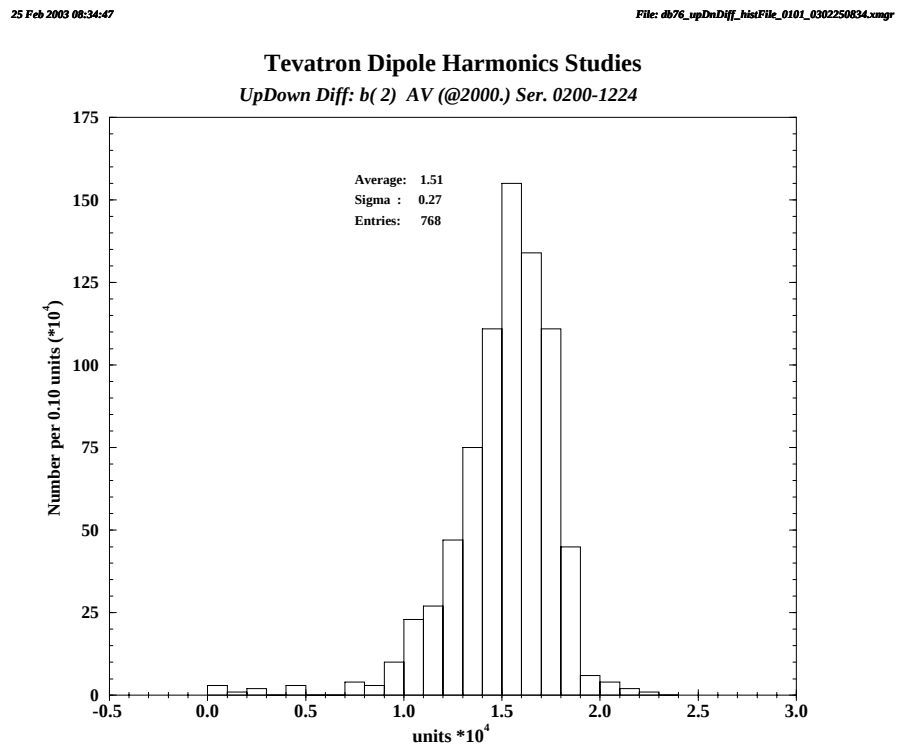

Figure 26: Tevatron dipole archival magnetic measurement data: Distribution of b_2 loop width (in units at 25.4 mm) at 2000 A of all Tevatron dipoles installed.

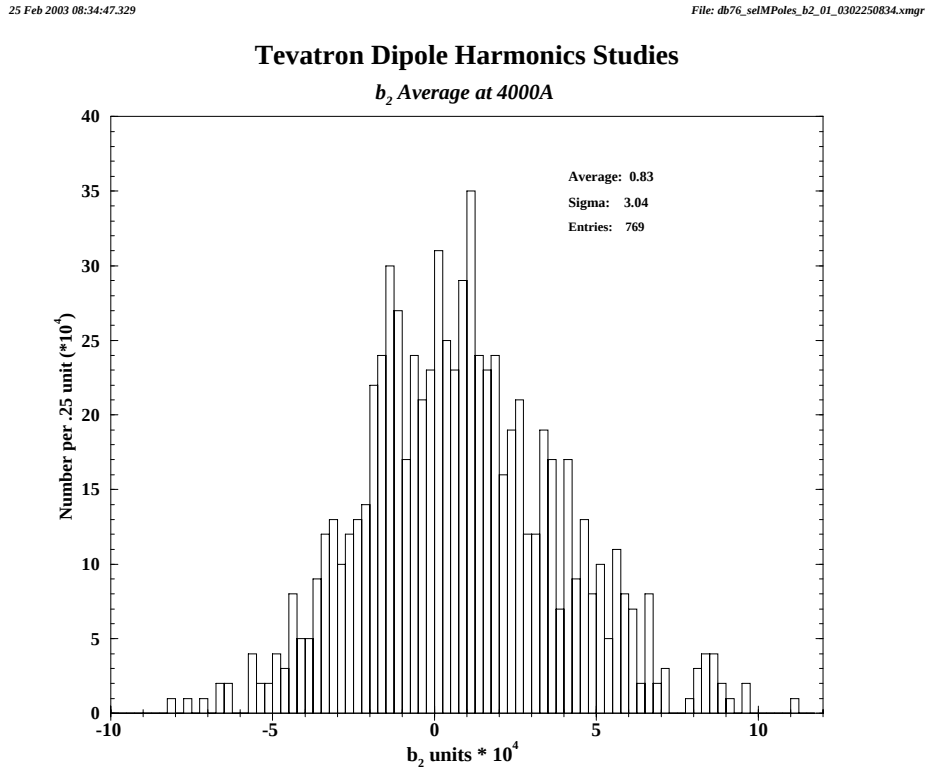

Figure 27: Tevatron dipole archival magnetic measurement data: Average b_2 (in units at 25.4 mm) of all Tevatron dipoles installed at 4000 A (~900 GeV beam energy).

APPENDIX 5

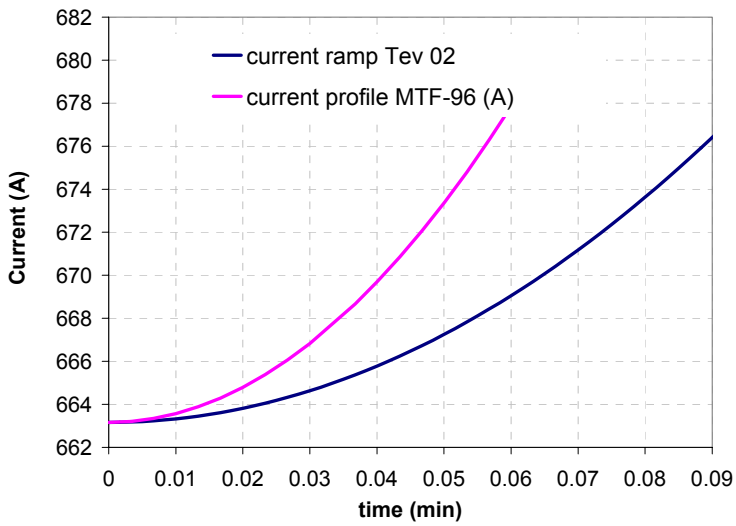

Figure 28: Current profiles for ramp from injection in the Tevatron today and the MTF measurements performed in 1996.

References

1 D.A. Herrup et al., "*Time Variations of Fields in Superconducting Magnets and their Effects on Accelerators*", Proceedings of the 1988 Applied Superconductivity Conference, IEEE Transactions on Magnetics, Vol. 25, No. 2, 1643-1646, March 1989 (also available as Fermilab Technical Memo TM-1543)

2 P. Bauer et al., *"Tevatron Dipole Magnetic Models, Part 1 – Static Fields"*, Fermilab, Technical Division, internal note TD-02-040, January 01

3 G. Annala et al., "*Tevatron Dipole Measurements at MTF*", write-up of 1996 magnetic measurements on magnets TC0504 and TC1052, http://www-bdnew.fnal.gov/tevatron/adcon/magnets.html

4 M. Martens, G. Annala, "*Chromaticity, Tune and Coupling Drift and Snapback Correction Algorithms in the Tevatron*", Fermilab/BD/Tev note Beams-doc-467, Feb. 24th, 2003, direct link: http://beamdocs.fnal.gov/cgi-bin/public/DocDB/ShowDocument?docid=467

5 P. Bauer, Fermilab-Technical Division, internal note, *"Historical Review of the Discovery of Dynamic Effects in Tevatron Magnets"*, TD-03-007, Feb. 2003

6 M. Martens, P. Bauer, D. Still, G. Annala, "*Measurement of the Average B2 Component in the Tevatron Dipole Magnets at the Start of the Energy Ramp*" Beams-Doc-478, March 2003

7 G. Velev, P. Bauer, "*Magnetic Measurements on Tevatron dipoles*", TD-note in preparation

8 J. Theilacker, personal communication

9 M. Xiao, personal communication

10 Courtesy of L. Bottura, Cern/LHC/MTA